Simulation of Brittle Collapse Mechanisms in Historical Masonry Using Sequentially Linear Analysis (SLA)

Manimaran Pari(✉) and Jan Rots

Delft University of Technology, Stevinweg 1, 2628 CN Delft, The Netherlands
m.pari@tudelft.nl

Abstract. Sequentially Linear Analysis (SLA) is known for robust and reliable finite element simulations of masonry constructions, often considered challenging because of the brittle behaviour of the masonry material. Herein a sequence of scaled linear analyses is performed with decreasing secant stiffness of one integration point per analysis, representing local damage increments. This procedure is especially suited to simulate highly nonlinear collapse mechanisms. In this article, a benchmark experiment on structural historical masonry is first chosen. This benchmark is simulated using SLA, using the micro-modelling approach, with linear blocks/bricks and nonlinear interfaces using a multi-surface interface model. The results are compared against those of the experiment, nonlinear finite element analysis, and the Discrete Element Method (DEM), good agreement is found with those of the experiment, and the collapse mechanisms are also captured in a robust manner.

Keywords: Sequentially Linear Analysis (SLA) · Robust simulations · Brittle failures · Multi-surface interface model · Micro-modelling

1 Introduction

Historical constructions are known to collapse in a rather brittle manner when subject to extreme loadings like torrential rains, earthquakes and extreme winds. Nonlinear finite element analyses, NLFEA, of such collapsing structures is a proven advanced numerical tool. However, traditional incremental-iterative solution procedures in NLFEA are often considered challenging because of the convergence troubles that arise owing to the softening behaviour of the masonry material [1]. This can be controlled using path following methods like arc-length control, at the expense of several trial runs, or other solution procedures like explicit dynamic methods. Alternatively, there exists a class of solution procedures based on the Sequentially Linear Analysis (SLA), to achieve robust and reliable finite element (FE) simulations, wherein a sequence of scaled linear analyses is performed with decreasing secant stiffness of one integration point per analysis, representing local damage increments. This procedure is a proven alternative for masonry analyses and is especially suited to simulate highly nonlinear collapse mechanisms.

Y. Endo and T. Hanazato (Eds.): SAHC 2023, RILEM Bookseries 46, pp. 603–616, 2024.
https://doi.org/10.1007/978-3-031-39450-8_50

In this article, a benchmark experiment in masonry showcasing collapse mechanism is chosen. This is simulated using SLA, with its latest constitutive and solver developments [2–4], in order to capture collapse mechanisms under non-proportional loading conditions. The case is modelled using the micro-modelling approach of masonry [5], differentiating the continuum into linear elastic bricks and potential failure planes represented by interface elements: along head and bed joints, and additionally, a potential vertical brick cracking plane in the middle of each brick (if necessary). Furthermore, a case-study of a pushover experiment presentative of historical masonry structure – the part of the cloister's facade of the Sao Vicente de Fora monastery in Lisbon [6, 7] is studied. The results of the SLA simulations are compared with those of an NLFEA and the Discrete Element Method (DEM) [8]. The paper first presents the SLA methodology and the constitutive model used therein, followed by the benchmark experiment and the simulation results. Finally, the historical masonry structure simulation results and conclusions are presented.

2 Sequentially Linear Analysis: Methodology

The Sequentially linear analysis (SLA), a non-incremental (total) solution approach [1], helps simulate the damage process in quasi-brittle materials by allowing for one damage event at a time. The crux of the approach relies on sequentially running linear analyses, i.e., an event-by-event approach, each of which identifies a critical integration point in the FE model with the maximum stress. The strength and stiffness of this critical point are then reduced based on a discretised step-wise constitutive relation called the saw-tooth law shown in Fig. 2. Thereafter, the linear analysis results, i.e., the displacements, forces, stresses and strains, are scaled using the critical load multiplier λ_{crit}, the least ratio of the allowable strength to the governing stress over all integration points. For a scalable load L, the load multiplier for each IP i and the overall critical load multiplier (minimum of all positive load multipliers) are defined as follows:

$$\lambda i(ft/\boldsymbol{\sigma} gov);\ \lambda crit = min(\lambda i);\ Lcrit = \lambda crit\, L \tag{1}$$

Herein, the nonlinear modelling of quasi brittle fracture is alleviated of multiple cracks attempting to survive and the use of secant stiffness makes the procedure additionally very robust. The sequence of linear analysis continues until a predefined termination criterion is reached.

A composite-interface formulation, previously proposed to be used in conjunction with the sequentially linear framework [2] is used herein. The failure surface (2D and 3D) shown in Fig. 1 has: (a) a tension-cut-off criterion coupled with a uniaxial tension softening law; (b) a compression-cap cut-off criterion, dependent purely on the normal traction, coupled with a uniaxial parabolic hardening–softening law; and (c) a step-wise secant Coulomb friction law which decouples the tension and shear modes, the dilatancy effects are neglected because of no coupling, i.e. the dilatancy angle $\psi = 0$, an assumption that yields good results for masonry structures in general [2]. Step-wise secant saw-tooth laws address all aforementioned uniaxial behaviour (See Fig. 2). For further details on the model the reader is referred to Reference [2].

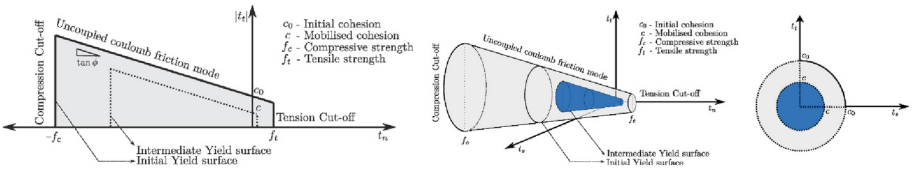

Fig. 1. Failure surface for the 2D line interfaces (left) and 3D planar interfaces (right)

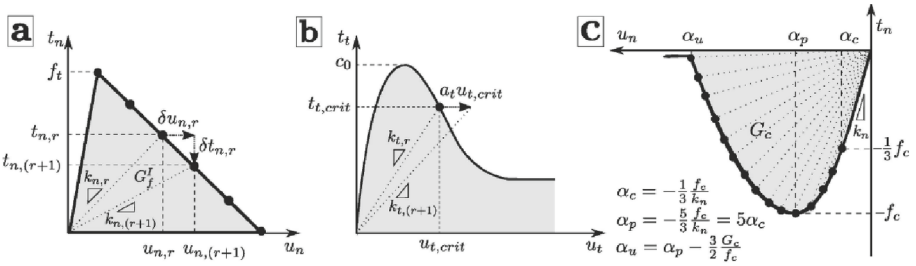

Fig. 2. Linear tension softening (a), cohesion softening (b) and compression hardening-softening (c) saw tooth constitutive laws

The critical load multiplier in SLA for non-proportional loading conditions involving a constant load, for e.g., deadweight, and a variable load like a wind load, is different from Eq. 1. In case of the interfaces for example, the tractions are expressed as the superposition of the tractions due to the constant and scaled variable loads as shown in Eq. (2) for each integration point *i*. The governing stress is then limited by the allowable strengths *f*, corresponding to the failure criterion, as shown in Eq. (3), such that only the critical integration point *i* lies on the failure surface while all non-critical points lie below it. These equations could apply for any of the failure possibilities i.e., cracking, crushing or shearing. As long as Eq. (3) holds, Eq. (4) applies at the global level. Contrarily, when Eq. (3) fails in a certain analysis step *j*, the procedure is steered into the *Intermittent Proportional Loading* (denoted by subscript *ipl* hereon) [9, 10] in the next step ($j + 1$), while implicitly reducing the constant load, as shown in Eq. (5a), (5b) to reinstate Eq. (3). Such regions indicate the need for multiple failures representing a sudden propagation of damage. Once the critical integration point and the load multiplier is determined, the strength and stiffness corresponding to the failure type is reduced stepwise, the linear analysis results are scaled, and the procedure moves to the next linear analysis. Alternatively, in an incremental version of SLA i.e., the Force-Release method [4], the non-proportional load path is discretised into a series of piece-wise proportional loading paths. Linear analyses are performed with load increments of a certain load vector, each of which may or may not lead to damage at a critical integration point *i* according to Eq. (6), wherein all quantities with Δ are the corresponding incremental values caused by the load increment. Upon damage, the stress from a damaged element is released gradually through a sequentially linear redistribution loop wherein the unbalanced forces due to the previous damage are applied as loads on the FE model, while all previously applied loads are kept constant, and other elements may be damaged. When the redistribution

loop does not lead to further damage, the response stays in equilibrium. Otherwise, it evolves through states of disequilibrium and eventually returns to equilibrium.

$$ti = ti, con + \lambda\, ti, var \tag{2}$$

$$(ti, con + \lambda ti, var) = f \wedge \forall i \neq k : (tk, con + \lambda tk, var) < f \tag{3}$$

$$Lcrit, j = \lambda con\, Lcon + \lambda var\, Lvar\, with\, \lambda con = 1\, and\, \lambda var = \lambda crit, j \tag{4}$$

$$\text{Lipl} = \text{Lcon} + \lambda\text{crit, (j} - 1)\ \text{Lvar and Lipl, j} = \lambda\text{crit, j Lipl} \tag{5}$$

$$(\text{ti} + \lambda\, \Delta\text{ti}) = \text{f} \wedge \forall\text{i} \neq \text{k} : (\text{tk} + \lambda\, \Delta\text{tk}) < \text{f} \tag{6}$$

3 Structural Masonry Benchmark

In this section, the validity of the sequentially linear approach in conjunction with the micro-modelling approach using the multi-surface interface constitutive model is revisited. The SLA study on the experiment on a solid clay brick masonry wall [2], tested by Raijmakers and Vermeltfoort [11, 12] and popularly used by fellow researchers as a benchmark case, is briefed upon.

3.1 Experiment and Finite Element Model

The solid clay brick masonry wall tested by Raijmakers and Vermeltfoort [11, 12], wall was made of 18 courses of bricks, with dimensions of 210 mm × 52 mm × 100 mm, and mortar layers of 10 mm thickness. The top and bottom courses of bricks were clamped to a steel beam to constrain the rotation along both edges, additionally preventing the free vertical movement of the top edge. The walls were loaded initially by an overburden pressure of 0.30 N/mm^2, followed by a monotonically increasing lateral load d applied under displacement control. The walls are discretised using the simplified micro-modelling strategy [5], wherein mortar joints and the brick–mortar interfaces are lumped together into a zero-thickness interface, and the bricks are extended to account for the mortar thickness. Appropriate boundary conditions are applied and the bricks are modelled using 4-noded iso-parametric plane stress elements (27.5 mm × 27.5 mm in size) with linear interpolation shape functions and a 2 × 2 Gaussian integration scheme. Zero-thickness interfaces are modelled using 2 + 2 noded interface elements in conjunction with a 2-point Newton–Cotes integration scheme. The FE model is as shown in the Fig. 3 alongside material properties listed in Table 1. For further details on the model, the reader is referred to Reference [2].

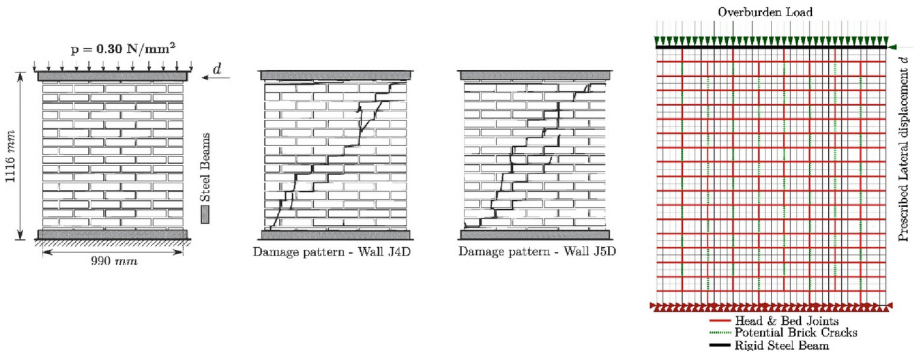

Fig. 3. Schematic representation of the experiment on solids clay brick masonry walls and the FE Model

3.2 SLA Results and Discussion

The wall firstly exhibits flexural failure which is visible as horizontal cracks along bed joints at the bottom-right and top-left corners of the wall (See Fig. 4). After the flexural cracks are fully developed (before 2 mm top displacement), compressive strut action results in a staggered step-like crack along the diagonal to the toe (left bottom corner) of the wall. This damage propagation includes both sliding failure along the bed joints, resulting in loss of shear stiffness, and tensile cracking along head joints, resulting in loss of both normal and shear stiffnesses. The fully developed flexural cracks and propagating diagonal step cracks at 2 mm top displacement are shown as tensile cracking and shear failure plots in Fig. 4. Furthermore, the stress flow into the toe of the wall leads to the onset of the crushing failure, which can be seen as loss of normal stiffness in the crushing plots of Fig. 4. The damage plots DmTeNN and DmCoNN indicate loss of normal stiffness due to cracking and crushing respectively. The DmTeSS damage plots indicate loss of shear stiffness which is either due to a pure-sliding failure or the damage based shear reduction associated with the cracking/crushing modes. All damage plots herein range from 0 to 1 which refer to undamaged and fully damaged cases for the corresponding failure criteria.

Upon further increase of the lateral displacement to 4 mm, the damage along the diagonal shear crack increases and localises, leading to a widening of the head joints and simultaneous sliding along bed joints, along the diagonal of the wall. Furthermore, the stepped crack also involves vertical splitting cracks through the bricks along the courses at mid-height of the wall, which often appear as sudden drops/instabilities in traditional NLFEA [5]. This is adequately captured by SLA. Simultaneously, the toe of the wall is completely crushed along half the length of an entire brick. This results in a clear drop of lateral capacity which is observed in the force–displacement curve, indicating structural collapse.

The case is also simulated using the Force-Release method and the results compare well with SLA and is mostly an envelope of the SLA response. There exists close similarity in the damage plots of the SLA and Force-Release simulations for continuum FE studies unlike lattice element models [4], and therefore Force-Release plots aren't

Table 1. FE Model parameters

Units	Parameters	Elastic	Compression	Tension	Shear
Bricks	Young's Modulus E_0 [GPa]	16.7			
	Poisson's ratio ν_0	0.15			
Brick Cracks	Normal stiffness k_n [N/mm^3]	10^6			
	Shear stiffness k_t [N/mm^3]	10^6			
	Tensile Strength f_t [MPa]			2	
	Fracture energy G_f^I [N/mm]			0.08	
	Saw-teeth discretisation factor			0.2	
	Softening relation			Linear	
	Shear retention factor β			Damage-based [10]	
Head & Bed Joints	Normal stiffness k_n [N/mm^3]	82			
	Shear stiffness k_t [N/mm^3]	36			
	Strength fc, ft, c_0 [MPa]		6.0	0.25	0.35
	Fracture energy G_c, G_f^I, G_f^{II} [N/mm]		1.8	0.018	0.125
	Saw-teeth discretisation factor		0.1	0.15	0.05
	Softening relation		Parabolic	Linear	Exponential
	Shear retention factor β		Damage-based [10]	Damage-based [10]	–

shown herein (refer [2]). The differences become apparent whenever SLA returns to the *Intermittent Proportional Loading* (IPL), wherein the last successful load combination is scaled proportionally to avoid violation of the constitutive law anywhere in the FE model. Under such conditions, the overburden load in SLA is implicitly reduced to enforce equilibrium during a quasi-static damage driven failure propagation. This becomes significant starting ~3.7 mm prescribed lateral displacement, marked as a yellow circle in the force-displacement plot of Fig. 4, indicating onset of collapse. The constant load drops to extremely low values through this region but is also recovered

immediately (Fig. 4), which appears as large snap-backs in the post-collapse region at prescribed lateral displacements around 4 mm. Since every damaged element's stress is released instantaneously in SLA, the neighbouring integration points of the critical integration point whose stresses are close to their respective allowable strengths subsequently become critical at a considerably lower load. In summary, the performance of the non-proportional loading strategy of SLA is successful in this problem leading to collapse, which in turn is described using its inherent redistribution procedure i.e., the IPL. On the other hand, these regions are simulated in disequilibrium using the Force-Release method appearing as instabilities or *drops* of load for a constant imposed displacement. The collapse mechanism herein is captured by both approaches adequately. However, the drop of load corresponding to the eventual instability is described by the SLA and the Force-Release methods in diametrically opposite ways, with regard to the time scales for the redistribution. This is in line with the differences observed between the approaches to typical explosive failure in the previous case studies [9], and is clear from how the loading is modified in case of SLA (Fig. 4) during collapse. SLA describes the entire collapse while maintaining equilibrium by reducing the constant load, while the Force-Release method addresses it using the avalanche of damage states in disequilibrium which appear as vertical drops of the capacity.

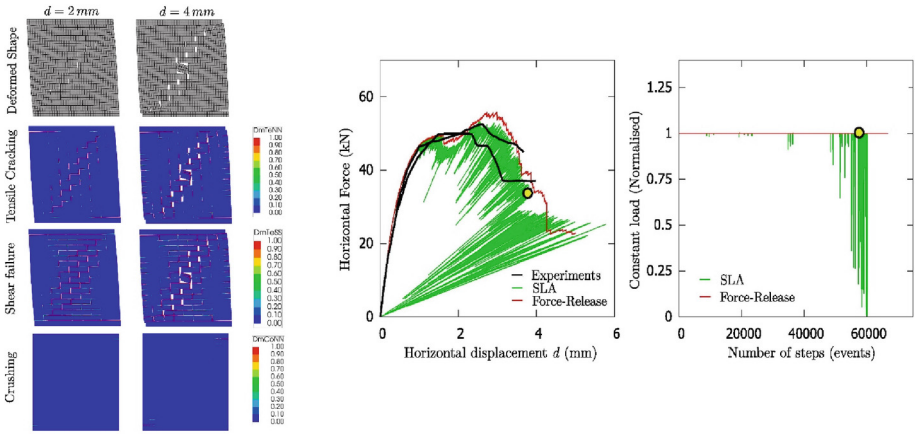

Fig. 4. The deformed profile, and damage plots indicating tensile, shear and crushing failures for the pushover study, with discrete cracking-shearing-crushing interfaces, using the SLA method at 2 mm and 4 mm prescribed lateral displacements. Force–displacement curves of the experiments compared against those of the SLA and the Force-Release simulations, and (b) the evolution of constant load of pre-compression during the simulations.

The suitability of the two sequentially linear methods depends on the type of experiment being simulated. Force-Release method is suitable for typical displacement-controlled experiments which actually exhibit instabilities. These would be consistent with the drops of loads observed in Force-Release simulations. On the other hand, it may not be suitable for physical processes which exhibit snap backs or for truly quasi-static

experiments. SLA is more preferable when the damage process zone is unique and controlled for quasi-static evolution in an experiment [9, 10]. However, for a Crack Mouth Opening Displacement (CMOD) controlled experiment with multiple cracking zones, SLA may also not be appropriate because it does not control a unique damage process zone as in the experiment, and contrarily may incorrectly decrease it due to release of previously applied loads while allowing the structure to relax. Force-Release method, in this case, may increase the CMOD due to the redistribution. In a quasi-static sequentially linear setup, a truly CMOD controlled experiment with multiple evolving damage zones can be appropriately simulated by the so-called *general* method [9]. For a detailed analysis on the applicability of the approaches, the reader is referred to References [9, 10].

4 Historical Masonry Benchmark

4.1 Experiment and Finite Element Model

Experiments on the behaviour of full-scale masonry structures representative of historical masonry, is very limited. Historical masonry are therefore usually analysed directly by first calibration and validation of numerical models based on experimental benchmarks on structural walls or facades. In this regard, the experiment conducted at the ELSA laboratory of the Joint Research Centre of the European Commission, on a full-scale model of part of the cloisters of the Sao Vicente de Fora monastery in Lisbon (Fig. 5) is unique. Details of the experimental findings are presented in Ref. [6] and the tested model features three stone block columns, two complete arches and two half arches, as shown in Fig. 5 [7].

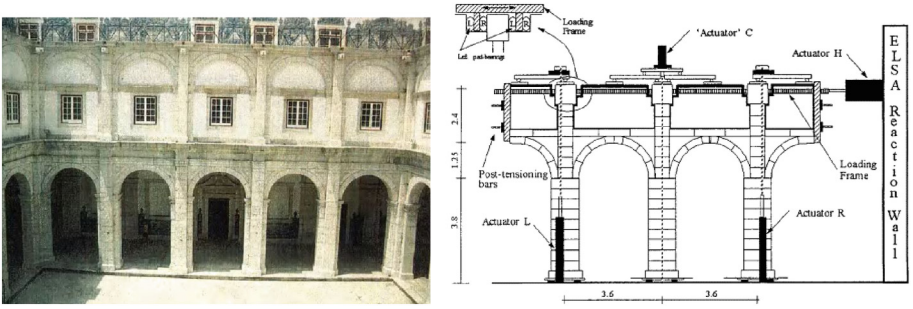

Fig. 5. Cloisters of the Sao Vicente de Fora monastery (internal view – left) and the experimental set-up (image from Reference [7] - right).

The experimental set-up is as shown in Fig. 5. The FE model is made using the simplified micro-modelling strategy [5] as in the previous section, wherein mortar joints and the stone block-mortar interfaces are lumped together into a zero-thickness interface, and the stone blocks are extended to account for the mortar thickness. The stone blocks are modelled linear elastically using 8-noded iso-parametric plane stress elements, roughly

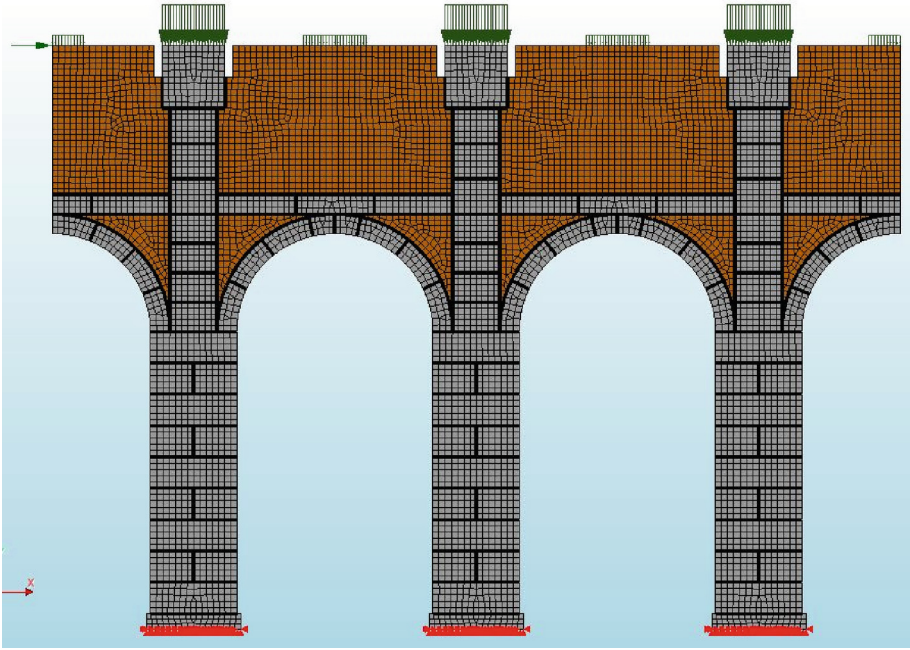

Fig. 6. FE micro-model of the structure showing head and bed joints in black, stone masonry in grey, infill brick masonry in brown, loads in dark green and the bottom supports in red.

75 mm in size with a 2 × 2 Gaussian integration scheme. The zero-thickness interfaces are modelled using 3 + 3 noded interface elements, in conjunction with a 3-point Newton–Cotes integration scheme. The infill brick masonry and the stone blocks are kept linear elastic. Material parameters are as shown in Table 2. The thickness of the wall is assumed to be 500 mm after a sensitivity analysis for initial stiffness and dead weight, as information on cross section is sparse. The boundary conditions that have been provided try to simulate the test setup as well as possible. The base nodes are pinned and the nodes at top of the two external pillars have been constrained to have equal vertical displacements. As far as loading is concerned, firstly vertical dead loads are applied so as to result in 400 kN per pillar/panel distributed in a 4/1 ratio, alongside self-weight. Secondly, prescribed displacements were applied to the top edge of the structure to simulate the static equivalence of seismic action. The structure is supported at the bottom in both horizontal and vertical direction to simulate the fixed boundary condition. Two analyses were run on the FE model. Firstly, a Sequentially linear analysis is performed. Secondly, for comparison purposes, a Non-Linear Finite Element Analysis (NLFEA) with the traditional incremental-iterative approach was done with the two loading stages. Lateral load was applied to a total of 30mm top displacements in 100 steps of 0.3mm, wherein the Newton Raphson iteration scheme that converges to an energy norm of 0.0001 was used. Aside the differences from the load application procedure, it is to be noted that the coulomb friction model with gapping criterion [14]

used in NLFEA has no cohesion/tension softening, while in SLA softening is allowed as described in Table 2 (Fig. 6).

Table 2. FE Model parameters

Units	Parameters	Elastic	Tension	Shear
Stone	Young's Modulus E_0 [GPa]	23		
	Poisson's ratio v_0	0.2		
	Self-Weight (kg/mm^3)	2500		
Brick infill	Young's Modulus E_0 [GPa]	2.3		
	Poisson's ratio v_0	0.2		
	Self-Weight (kg/mm^3)	2500		
Head & Bed Joints	Normal stiffness k_n [N/mm^3]	115		
	Shear stiffness k_t [N/mm^3]	47.9		
	Strength f_t, c_0 [MPa]		0.1	0.1
	Fracture energy G_f^I, G_f^{II} [N/mm]		0.1	10
	Saw-teeth discretisation factor		0.2	0.05
	Softening relation		Linear	Exponential
	Shear retention factor β		Damage-based [10]	–

4.2 Results and Discussion

The results from SLA on the structure are compared against the experimental monotonic envelope and other numerical simulations in Fig. 7. SLA slightly underestimates the ultimate strength but with regard to the initial stiffness degradation and damage formation, the result is appreciable. The SLA curve is qualitatively quite comparable and reasonable in relation to similar block-based modelling results from literature i.e. the joint model in CASTEM 2000 or the distinct element method with deformable bocks [13] and also the NLFEA analysis performed herein. The differences arise owing to the inherent differences in the approaches. CASTEM 2000 joint model is assumed to follow a simple elasto-plastic Coulomb friction law with no cohesion or tensile strength, while SLA allows for both cohesion and tensile softening. The damage pattern from the CASTEM model shown in Fig. 10 shows concentration of deformation in joints as

expected and is somewhat similar to the SLA damage pattern in Fig. 9. SLA, however, allows for asymmetric failure localisation and propagation unlike the traditional solution procedure and this is evident in the large opening and sliding damage close to the left column/infill interface, while in CASTEM the damage is more distributed. NLFEA results also are similar to SLA but suffer from convergence issues typical of implicit solvers (unconverged points are shown in Fig. 7.), and this alongside the differences in the constitutive modelling i.e., no softening in tension/cohesion give rise to the disparity in damage shown in Fig. 11 for NLFEA. DEM damage plots/results were not shown in the work of reference [13] and are therefore not compared herein. In summary, the performance of SLA seems quite appreciable. With regard to the non-proportional loading algorithm, as shown in Fig. 8, the constant load of overburden and self-weight are applied over 1000 steps initially involving damage before reaching the full value of unity. Thereafter, when the lateral load is applied, the drops in constant load seen in Fig. 8 correspond to the intermittent proportional loading, necessary during highly nonlinear regions of the structural response, when a linearly scaled combination of loads is not possible anymore. This has been previously shown to be acceptable as long as the loads don't completely start to decrease to zero which is a sign of the onset of structural collapse [9]. Therefore, the current SLA simulation is appreciable from this point of view considering that this has been an ongoing topic of debate [9, 10].

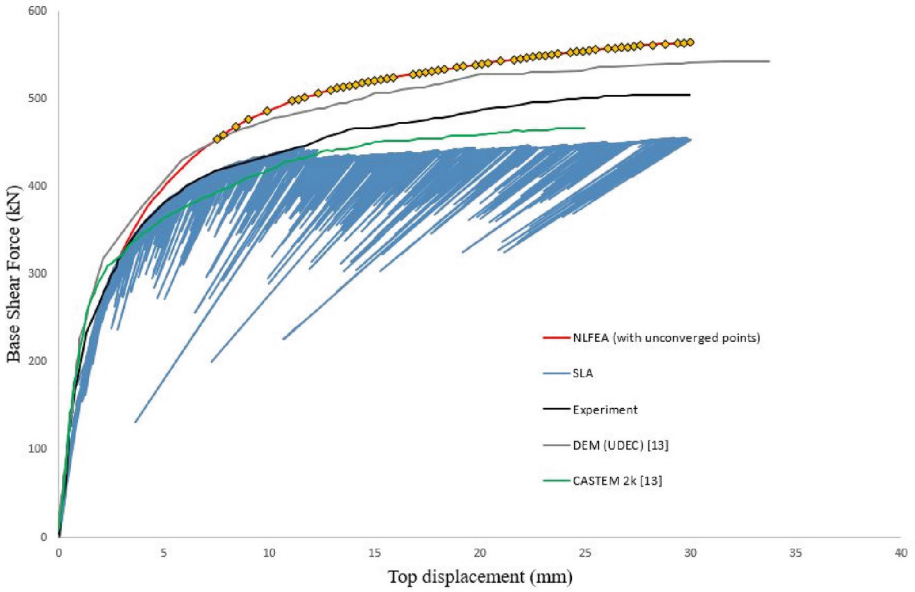

Fig. 7. Experimental and numerical curves from this study (NLFEA, SLA) and from literature (DEM and CASTEM) [13].

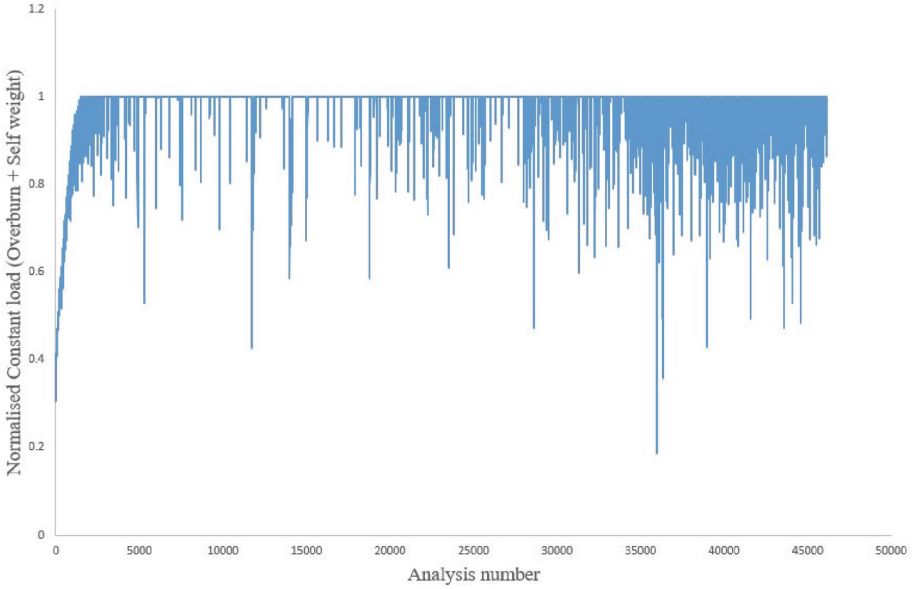

Fig. 8. Evolution and fluctuation of the first load i.e., the overburden and self-weight during SLA to allow for admissible damage

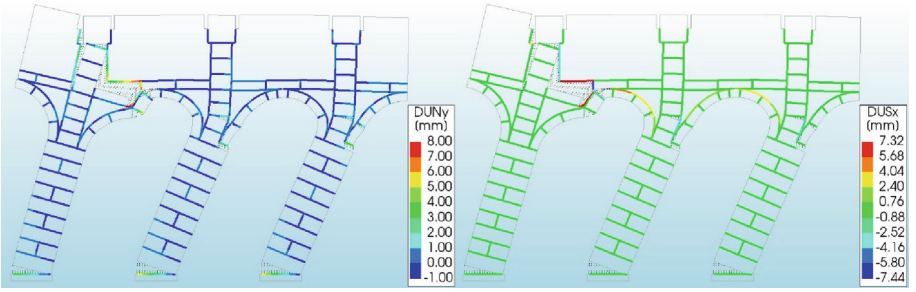

Fig. 9. Normal and tangential displacements (Left-Opening and Right-sliding) at the interfaces for the SLA model

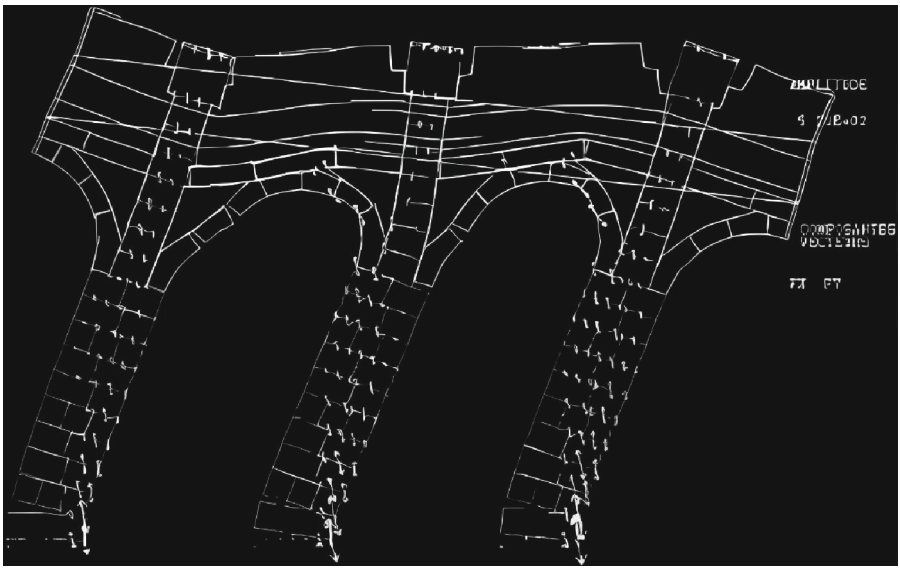

Fig. 10. CASTEM 2000 displaced mesh [13]

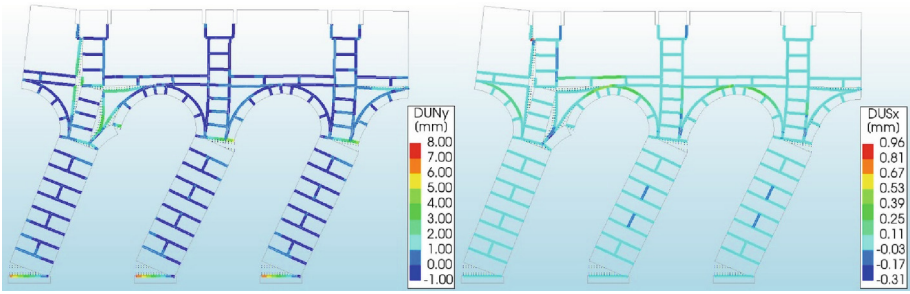

Fig. 11. Normal and tangential displacements (Left-Opening and Right-sliding) at the interfaces for the NLFEA model

5 Conclusions

This article presents an overview of the sequentially linear analysis approach, in conjunction with a composite interface formulation, for micro-modelling or block-based approach to the analysis of masonry structures. A structural historical masonry benchmark is chosen and simulated using SLA quite appreciably. This shows potential of the method, especially in highly nonlinear and brittle collapse mechanisms, to provide results in a numerically robust manner compared to the traditional incremental iterative solution in the finite element method. The method is also comparable to block-based modelling strategies in literature, while being a more robust alternative. The method is currently being investigated for geometrically nonlinear, plasticity and other loading/stress history-related problems.

References

1. Rots, J.G., Invernizzi, S.: Regularized sequentially linear saw-tooth softening model. Int. J. Numer. Anal. Meth. Geomech. **28**(7–8), 821–856 (2004)
2. Pari, M., Van de Graaf, A.V., Hendriks, M.A.N., Rots, J.G.: A multi-surface interface model for sequentially linear methods to analyse masonry structures. Eng. Struct. **238**, 112123 (2021)
3. Pari, M., Swart, W., van Gijzen, M.B., Hendriks, M.A.N., Rots, J.G.: Two solution strategies to improve the computational performance of sequentially linear analysis for quasi-brittle structures. Int. J. Numer. Meth. Eng. **121**(10), 2128–2146 (2020)
4. Eliáš, J., Frantík, P., Vořechovský, M.: Improved sequentially linear solution procedure. Eng. Fract. Mech. **77**(12), 2263–2276 (2010)
5. Lourenco, P.B.: Computational strategies for masonry structures. Ph.D. thesis, Delft University of Technology (1996)
6. Pinto, A.V., et al.: Laboratory tests on full scale monument. In: Proceedings of the 11th European Conference on Earthquake Engineering, Paris (France) (1998)
7. Pegon, P., Pinto, A.V.: Seismic Study of Monumental Structures Structural Analysis, Modelling and Definition of Experimental Model. Report EUR 16387 EN, European Laboratory for Structural Assessment (1996)
8. Pulatsu, B., Bretas, E.M., Lourenco, P.B.: Discrete element modeling of masonry structures: validation and application. Geomech. Eng. **11**(4), 563–582 (2016)
9. Pari, M., Hendriks, M.A.N., Rots, J.G.: Non-proportional loading in sequentially linear solution procedures for quasi-brittle fracture: a comparison and perspective on the mechanism of stress redistribution. Eng. Fract. Mech. **230**, 106960 (2020)
10. Pari, M.: Simulating quasi-brittle failure in structures using sequentially linear methods: Studies on non-proportional loading, constitutive modelling, and computational efficiency. Ph.D. thesis, Delft University of Technology (2020)
11. Raijmakers, T., Vermeltfoort, A.T.: Deformation controlled tests in masonry shear walls, Report B-92-1156, TNO-Bouw, Delft (1992)
12. Raijmakers, T., Vermeltfoort, A.T.: Deformation controlled tests in masonry shear walls: Part 2, Report TUE/BKO/93.08, Eindhoven university of technology (1993)
13. Giordano, A., Mele, E., De Luca, A.: Modelling of historical masonry structures: comparison of different approaches through a case study. Eng. Struct. **24**(8), 1057–1069 (2002)
14. Ferrera, D.: Diana User's Manual, Release 10.5. DIANA FEA BV (2022)